REAL TIME MONITORING OF MEAT FRESHNESS BASED ON NATURAL RESOURCES

EMINE ARMAN KANDIRMAZ,[*] URŠKA KAVČIČ,[**] ARIF OZCAN,[*]
GREGOR LAVRIČ[**] and IGOR KARLOVITS[***]

[*]*Marmara University, Faculty of Applied Sciences, Department of Printing Technologies, Kartal Istanbul, 34865, Turkey*
[**]*Pulp and Paper Institute, Department of Graphics and Packaging, Bogišićeva Ulica 8, 1000 Ljubljana, Slovenia*
[***]*Danfoss Trata d.o.o., Šentvid, Slovenia*
✉ *Corresponding author: E. Arman Kandirmaz, earman@marmara.edu.tr*

Received October 7, 2025

Food spoilage leads to both food waste and consumer health damage. Smart packaging systems inform the consumer about food spoilage and prevent food waste by consuming at the right time. Considering this and consumers' increasing preference for natural packaging materials for food products, in this study, it was aimed to produce smart packaging elements using naturally sourced cellulose derivatives and black carrot anthocyanins. Two types of nanocelluloses, namely bacterial nanocellulose (BNC) and TEMPO-oxidized cellulose nanofibrils (CNF), were synthesized from natural resources using different production methods. Black carrot was used to extract anthocyanin, a pH-responsive pigment. The attenuated total reflectance Fourier transform infrared (ATR-FTIR) spectroscopy was used to examine the chemical structures of BNC, CNF, and anthocyanin. The total anthocyanin content (TAC) in the black carrot extract was determined by UV spectroscopy. Thus, it was concluded that the colored substance obtained from black carrots had the cyanine 3-O-glucoside structure and its total anthocyanin content was 469±35 mg/100 g. Also, the color changes of anthocyanin in response to pH alterations were investigated.
Hydrogels were prepared based on BNC and CNF, separately, with Zn^{2+} used as crosslinker, and then these hydrogels were impregnated with the anthocyanin dye. Using ATR-FTIR, the chemical structure of the hydrogels loaded with anthocyanins was examined. Also, their swelling index was calculated and it was noted that BNC had a 15% higher swelling index. The morphology of the hydrogels was investigated using scanning electron microscopy (SEM).
Then, printable hydrogel suspensions were prepared from BNC, CNF, and anthocyanins, to develop intelligent pH-sensitive labels. These suspensions were used to print on paper using the screen-printing technique. An X-Rite spectrophotometer was used to analyze the color characteristics of the printed hydrogel suspensions in both basic and neutral settings. The cumulative release of anthocyanin from the CNF and BNC-based smart labels in ethyl alcohol was also examined in this work. It was determined that the anthocyanin released from BNC hydrogel was 3% higher than from CNF. The ability of these novel colorimetric freshness indicator labels to identify deterioration in minced beef was evaluated. It was observed that, with the change of ambient pH, the color changes of the printed labels can be detected both spectrally and visually. Thus, the color of the hydrogel ink on the labels changed from pink/purple to blue as the meat deteriorated, indicating the potential of these smart labels as spoilage indicators. According to the study's findings, these smart labels can serve as useful freshness labels for meat products, providing a useful application for materials derived from natural resources and advancing environmentally friendly packaging technology.

Keywords: freshness indicator, nanocellulose, smart label, hydrogel, anthocyanin

INTRODUCTION

The importance of food and food safety has increased in the modern era due to supply chain issues, wars, rising illnesses, and environmental issues. Around the world, smart packaging systems are widely used to guarantee food safety. Large-scale commercial techniques are employed for this, but they are expensive and necessitate the involvement of experienced personnel.[1,2] In addition, consumers are now curious about the freshness or spoilage of the product when choosing products in the market. One of the subjects examined is the real-time status detection of food

in the market prior to reaching the final consumer.[3] Foods, particularly meat and dairy products, are susceptible to spoiling and external influences due to their nature, surface structure, and processing methods.[4] Food packaging applications are the best systems for real-time monitoring. It is anticipated that these applications will offer real-time information without raising the price of the product, harming its structure, or endangering human health. The food and packaging sector have also been impacted by changes in consumption patterns, industrial advancements, and trends. As a result, systems have been created to track every step of the food production process, from the farm to the kitchen. These systems are often known as intelligent and active packaging systems.[5-7]

Active packaging refers to systems that extend product safety and shelf life by creating a barrier around food. These can be releasing systems that release ethanol, antioxidants, or antimicrobials, or they can be absorption systems that remove oxygen, ethylene, carbon dioxide, or moisture. On the other hand, smart packaging systems, which are increasingly used especially in pharmaceutical and food products, stand out. Without coming into contact with the product, these systems offer information about it or its surroundings, allowing for the control of product conditions. In this way, consumers can obtain the information they need about the product, and the manufacturer can easily monitor the product. With these systems, the presence of microorganisms, oxygen and temperature levels can be monitored.[8-10] Nowadays, the use of time, temperature, freshness (pH) and gas sensors has become widespread in the market.[11]

Freshness indicators are a type of acid-base indicators and are systems that react by being affected by the pH of the environment. In this way, they are smart packaging applications that identify the product's level of freshness or spoiling, allow monitoring and alerting the customer.[12] When the food product begins to lose its freshness, structural microbial growth begins and as a result, organic acids, volatile nitrogen compounds and carbon dioxide appear, and as a result, the chemical structure of the product begins to change. Systems that reveal the reaction here as a color change are preferred due to their easy perception, simplicity, and appearance. These simple-looking colorimetric indicators can detect changes according to the structure of the food (amines, ethanol, ammonia, pH, *etc*.).[13,14] These devices make it simple to see pH variations, particularly when meat products' chemical structures deteriorate. pH-based freshness indicators work with two basic components, these are the pH-sensitive halochromic dye and the polymer matrix that stabilizes this dye.[15] Despite the development of numerous pH-sensitive indicators, natural dyes that are biocompatible have gained more attention.[16] The color of plants generally results from anthocyanins, flavonols, xanthine, flavones, and azo structures in their structures, and some of them are pH sensitive.[8] The indicators' color spectrum is created based on how the food product's pH changes. As a result, pH indicators provide precise and reliable data for monitoring the freshness of food.[17,18] Anthocyanins are important as pH indicators because they can be found in plants, are water soluble and are sensitive to pH.[19-21] Grape-based ingredients[22-27] have been developed as pH-based indicators for different food products thanks to the anthocyanins they contain. Additionally, *Echium amoenum*,[28] red cabbage,[16] black carrot,[29,30] black bean[16] and *Vitis vinifera* varieties[31] can be used as a freshness indicator thanks to their anthocyanin structures.

The pH-sensitive halochromic dye must remain stable and the polymer used to support it must be compatible with the halochromic dye. In this sense, it is possible to come across a wide variety of applications. Smart films with excellent color sensitivity function were produced by blending anthocyanins extracted from purple sweet potatoes with curcumin,[32] bromothymol blue,[33,34] and methyl red.[35]

Most colorimetric indicators typically operate by changing pH depending on the solubility of target chemicals in water.[36] However, the sensitivity of such indicators may diminish if the package has a limited moisture environment, or the carrier has poor hygroscopicity.[37] Moisture and color change in foods affect pH sensitivity and effectiveness. Therefore, very hydrophilic, or water-containing hydrogels should be utilized in indicator manufacture to enhance the color response of pH-sensitive dyes to target compounds produced during food decomposition.

Hydrogels based on natural polymers are becoming more and more popular due to their benefits in terms of biodegradability and biocompatibility. Since cellulose and its derivatives are renewable and contain a large number of hydroxyl groups, they are increasingly being used in the creation of hydrogels.[38,39] Interest in nanocellulose-based hydrogels has increased due to their impressive structure and the properties

they exhibit.[40] Because of their high hydroxyl group content, bacterial nanocellulose (BNC), cellulose nanofibrils (CNF), and cellulose nanocrystals (CNC) have several desirable qualities, including excellent mechanical strength, outstanding biocompatibility, and highly reactive surfaces. Additionally, it can enhance the smart film's anthocyanins' color stability.[41,42] BNC is an environmentally friendly nanostructured biomaterial with high purity, high porosity and high mechanical properties.[43]

Printing systems are needed to produce smart labels with a cheap and sustainable system. The screen printing technology has advantages over other printing systems since it can print on a wide variety of substrates, is quick and simple to process, and allows for flexibility in modifying the thickness of the ink layer. The elimination of surface compatibility problems of natural materials and the elimination of low color intensity with high ink film thickness make screen printing a candidate method for smart labels.

In this study, nanocellulose was produced from Japanese knotweed, an invasive plant commonly found in Slovenia. In this way, it was aimed to reduce the dependence on valuable resources such as trees. Moreover, the produced nanocellulose will replace the petroleum-based polymers traditionally used in ink formulations, in line with the increasing environmental concerns regarding the use of fossil fuel-derived materials. The need for food protection and monitoring is increasing due to concerns such as decreasing food resources, increasing population and increasing awareness about nutrition. For this reason, the study planned to develop completely natural smart labels using anthocyanins (plant-based compounds) of natural origin to monitor food shelf life, and thus, it is foreseen that food products will be consumed within the optimum time frame. For this purpose, screen printing was performed by applying equal ink film thickness and labels were produced. The approach aimed to achieve both original and sustainable smart label production by integrating sustainable materials and innovative technologies, which distinguishes this research from the existing literature in the field.

In this study, the BNC used was prepared from a by-product that is generated during the traditional vinegar production process (mother of vinegar). In this way, sustainable and circular use of a by-product from the industry was demonstrated. For the CNF, the lignified stems of the invasive non-native plant Japanese knotweed, which poses a serious threat to native plant species in Central Europe, were used as the raw material. By converting an invasive plant into value-added products, we are helping the environment in several ways: we avoid using wood, and at the same time, we contribute to eliminating this species from the ecosystem.

EXPERIMENTAL

Materials

The black carrot and minced beef used in food degradation tests were purchased from a local market in Turkey. Zinc chloride (reagent grade, ≥98%) ($ZnCl_2$), sorbitol (≥98%) ($C_6H_{14}O_6$), ethyl alcohol (≥97%) (C_2H_5OH), sodium chlorite (80%) ($NaClO_2$), sodium hypochlorite (reagent grade, 10-15%) (NaClO), hydrochloric acid (ACS reagent, 37%) (HCl), glacial acetic acid (ACS reagent, ≥99.7%) (CH_3CO_2H), sodium bromide (ACS reagent, ≥99.0%) (NaBr), TEMPO reagent (98%) ($C_9H_{18}NO$), sodium hypochlorite (reagent grade, available chlorine 10-15%) (NaClO), sodium hydroxide (ACS reagent, ≥97.0%, pellets) (NaOH) were purchased from Sigma-Aldrich (Germany). The source of BNC will be the cellulose-rich biofilm (mother of vinegar), obtained from Slovenia local vinegar producers. Japanese knotweed was locally available in Slovenia.

Methods

BNC and CNF synthesis

The BNC used in this study was obtained from mother of vinegar, as described in the literature.[44] CNF was obtained from Japanese knotweed (*Reynoutria japonica)* stems, following the procedure described earlier.[45]

BNC and CNF hydrogel production

Hydrogels can be produced due to the hydrogen bonds formed between the hydroxyl groups on nanocelluloses. Zinc ions added to the reaction medium interact with the negatively charged functional groups (*e.g.*, carboxylate or hydroxyl groups) on the nanocellulose. These interactions help the polymer chains to connect to each other and form a network structure.

BNC and CNF hydrogels were prepared with $ZnCl_2$ (20%). During the preparation, 20% (w/v) $ZnCl_2$ was added dropwise into solutions containing 5% nanocellulose. A Teflon mold was used to shape the hydrogel. $ZnCl_2$ was carefully dropped from the edges. The added [Zn+] concentration was set to 0.1 mol/L. When the dripping process was completed, it was left unmoved overnight for the formation of hydrogels. Zinc ions acted as crosslinkers and hydrogels were obtained. The resulting hydrogel was washed with distilled water to remove unreacted zinc ions.[43]

The microstructures of the hydrogel samples were observed using a Philips XL30 model scanning electron

microscope. To fix the samples to the sample trays using, conductive adhesive tape (EMS CCC Carbon Adhesive for SEM Specimen Mounting EMS 12664) was used. Subsequently, samples were coated with platinum under vacuum conditions. The observations were conducted at an accelerating voltage of 10 kV and a magnification level of 100X.

Anthocyanin extraction from black carrot

Black carrot, a natural pigment source, was bought from a nearby market and kept at 4 °C until needed. The black carrots used in the study were first cleaned and then grated. After adding 10 g of black carrot pieces to a 1000 mL ethanol/water (4:1) mixture, the mixture was agitated for two hours at room temperature (23-25 °C) using a mechanical mixer set at 200 rpm. The liquid portion of the mixture, containing the active dye, was filtered. The solvents in the dye solution were eliminated by vacuum drying at 40 °C, with an evaporator operating at 1500 rpm. Then, it was subjected to ultracentrifugation at 13,500 rpm for ten minutes and vacuum drying at room temperature.

The chemical structure of the produced solid natural dyes was characterized with a Perkin-Elmer Spectrum 100 ATR-FTIR spectrophotometer (650-4000 cm^{-1} wavelength range).

The color changes caused by the pH change of the obtained dyestuffs were detected by a Shimadzu UV-visible spectrophotometer in the range of 380-800 nm.

Total anthocyanin content of the extract was determined according to literature.[46] First, absorbance values were read at 657 nm and 530 nm, using a Shimadzu UV-visible spectrophotometer. Then, the net absorbance (A_{net}) was calculated according to Equation (1):

$$A_{net} = A_{530} - 0.25A_{657} \quad (1)$$

In the spectrophotometric method anthocyanin was expressed as cyanidin-3-glucoside (cyd-3-glc) equivalents (cyanidin-3-glucoside molecular weight of 449.1 g/mol and extinction coefficient of 29,600, *DF* – dilution factor, *V* – total volume (mL), *Wt* – sample weight (*g*)). The conversion of the amount of anthocyanin from the amount of cyanidin 3 glycoside was determined according to Equation (2):

$$Anthocyanin\left(\frac{mg}{g}\right) = \frac{A_{net}}{29600} \cdot MW \cdot DF \cdot \frac{V}{Wt} \quad (2)$$

Anthocyanin absorption into hydrogels

The anthocyanins extracted in the previous sections were used as colorants, and were loaded into bacterial nanocellulose and cellulose nanofibril hydrogels. The natural active dye water solutions were first adjusted to a pH of 7, and then the hydrogels were immersed into the dye solution for 24 h. Afterwards, the dyed hydrogels were removed, and the wet surface was blotted with filter paper.

The hydrogels' swelling index (*SI*) was calculated using gravimetric analysis. In short, square-shaped sections of the hydrogel (three pieces of each) were heated at 70 °C for 24 h to obtain their initial dry weight (*M1*). After that, each dried sample was immersed in 20 mL of deionized water at 30 °C for 24 h, while being stirred. The samples were taken out and weighed after being dried with filter paper in order to determine the moist weight (*M2*). In the end, *SI* (%) were determined using Equation (3):

$$SI\ (\%) = [(M2 - M1) / M1] \times 100 \quad (3)$$

Three duplicates of the tests were conducted.

Preparation of printable anthocyanin-loaded hydrogel suspensions and printing

For use in screen printing, hydrogel suspensions (Table 1) were prepared. The concentration of nanocellulose fibrils and bacterial nanocellulose used as binders was reduced to 3% (w/w), and the amount of zinc was reduced by 4 times in order to provide less cross-linking. To increase the stabilization of the natural dye, 0.1% sorbitol was added to the medium. The viscosity of the produced suspensions was measured and adjusted to 1.00 Pa·s.[47]

Table 1
Printable hydrogel suspensions

	PHS 1	PHS 2
CNF	3%	-
BNC	-	3%
$ZnCl_2$	0.2%	0.2%
Sorbitol	0.1%	0.1%
Anthocyanin	2%	2%
Water	Viscosity adjusted to 1.00 Pa.s	

Thus, two different hydrogel suspensions were obtained (BNC/anthocyanin and CNF/anthocyanin), and were used as inks to print on an 80 g/m^2 paper with an Arus semi-automatic screen printing machine (printing parameters: 77 tpc weaving density, 75º squeegee angle and 75 shore squeegee hardness).

Characterization of prints

The X-Rite eXact hand-held spectrophotometer was used to examine the prints' color characteristics in accordance with ISO 13655:2017. A D50 light source, a 2° observer, a polarized filter, and a 0/45-degree geometry were used for the measurements, which were

conducted in the 400–700 nm spectral range. The difference between the colors of the different prints were calculated according to the CIE ΔE 2000 color-difference Equation (4) ISO 11664-6:2014. Calculations were made by taking the average of five measurements. *ΔL**, *Δa**, *Δb**: Difference in *L**, *a**, and *b** values between specimen color and target color. Lightness is represented by the *L** axis, which ranges from white to black. The red area is connected to the green by the *a** axis, while the *b** axis runs from yellow to blue.

$$\Delta E_{00} = \sqrt{\left(\frac{\Delta L'}{k_L S_L}\right)^2 + \left(\frac{\Delta C'}{k_C S_C}\right)^2 + \left(\frac{\Delta H'}{k_H S_H}\right)^2 + R_T \frac{\Delta C'}{k_C S_C}\frac{\Delta H'}{k_H S_H}} \quad (4)$$

where *ΔL**, *ΔC**, and *ΔH** are the CIE*L*a*b** metric lightness, chroma, and hue differences, respectively, calculated between the standard and the sample in a pair, *ΔR* is an interactive term between chroma and hue differences. The *SL*, *SC*, and *SH* are the weighting functions for the lightness, chroma, and hue components, respectively. The values calculated for these functions vary according to the positions of the sample pair being considered in CIE*L*a*b** color space. The *kL*, *kC*, and *kH* values are the parametric factors to be adjusted according to different viewing parameters, such as textures, backgrounds, separations, *etc*., for the lightness, chroma, and hue components, respectively.[48]

The nanocellulose-based hydrogel labels were tested for their affinity for anthocyanins using a color release test. After being submerged in 30 mL of varying polarity food simulants (0%, 10%, 50%, or 95% ethanol in distilled water), each hydrogel label was gently shaken for four hours. The absorbance of the label solutions was then measured using a UV-vis spectrophotometer at predefined intervals of time (15, 30, 60, 90, 120, 180, and 240 min).

Identification of minced beef freshness using the prepared smart labels

At this stage, the ability of the hydrogel-based smart labels to detect minced beef spoilage was investigated. For this purpose, 50 g of freshly purchased minced beef was placed in glass containers. The glass containers were completely sealed with linear low-density polyethylene films, and the indicator labels were fixed inside, in an airtight manner. The glass containers were stored in the refrigerator at 4 °C ± 2 and at room temperature at 18 °C ± 2. Changes due to degradation were examined both visually and spectrophotometrically. The X-Rite eXact hand-held spectrophotometer was used to detect changes according to the ISO 12647-2:2013 standard (with a D50 light source, 2° observer angle, polarizing filter, 0/45 degree geometry, in the 400 nm to 700 nm spectral range). CIE *L**, *a**, *b** values were measured at the beginning and for 7 days to quantitatively detect color changes on the indicator labels, according to the literature.[49] The average of the measurements taken on five different locations on the labels was calculated. The overall color difference was determined using the CIE technique, and Equation (4) was utilized to determine the color change (*ΔE_{00}*).

RESULTS AND DISCUSSION

Bacterial nanocellulose and cellulose nanofibrils were successfully produced by the methods described above. The chemical structure elucidation of the produced BNC and CNF molecules was performed by ATR-FTIR, and their spectra are shown in Figure 1. The ATR-FTIR spectra of CNF and BNC exhibited several significant differences that can be directly attributed to the TEMPO oxidation process. Both spectra showed a broad band at ~3340 cm^{-1} corresponding to O–H stretching vibrations; however, this band was more pronounced in BNC, suggesting a denser hydrogen-bonding network, which correlates with its higher swelling index. The bands at 2820–2900 cm^{-1} were assigned to the symmetric and asymmetric stretching of CH groups, while the absence of a peak at 1740 cm^{-1} confirmed the complete removal of hemicelluloses and lignin. A peak at ~1640 cm^{-1} was attributed to the bending vibrations of absorbed water. Unlike BNC, CNFs displayed a distinct peak at 1610 cm^{-1}, which corresponds to the carboxylate groups introduced during TEMPO oxidation. The presence of these negatively charged functional groups indicates increased surface hydrophilicity and reactivity of CNFs, consistent with their higher chemical accessibility compared to BNC.[50,51] Additionally, variations in the 1040–1050 cm^{-1} region reflected changes in C–O–C stretching of pyranose rings and glycosidic linkages, suggesting partial modification of cellulose chains in CNFs.[52] The glycosidic bonds were further confirmed by the band at 890 cm^{-1}. Overall, these spectral shifts and intensity variations demonstrate that, while BNC retains a more native cellulose structure with stronger hydrogen bonding, CNFs undergo substantial chemical modifications due to TEMPO oxidation. These structural alterations explain the distinct functional behaviors observed between CNF and BNC, particularly in hydrogel formation and anthocyanin loading, and are consistent with the literature.[50-52]

Natural pigment was extracted from black carrot. The chemical structure of the extract was examined by ATR-FTIR and is shown in Figure 2. When examining the spectrum, the planar deformation peak of C-H at 980 cm^{-1}, the C-H peak of aromatic ring at 1071 cm^{-1}, the C=O stretching peak of benzopyran ring at 1445 cm^{-1}, the C=C stretching peak in aromatic ring at 1590 cm^{-1}, the

stretching peak of pyran ring at 1235 cm^{-1}, the C-O angular deformation peak of phenols at 1335 cm^{-1}, the symmetric and asymmetric C-H vibration at 2830 and 2932 cm^{-1}, respectively, and the O-H stretching vibration at 3396 cm^{-1} can be clearly seen. These data are consistent with the literature.[53]

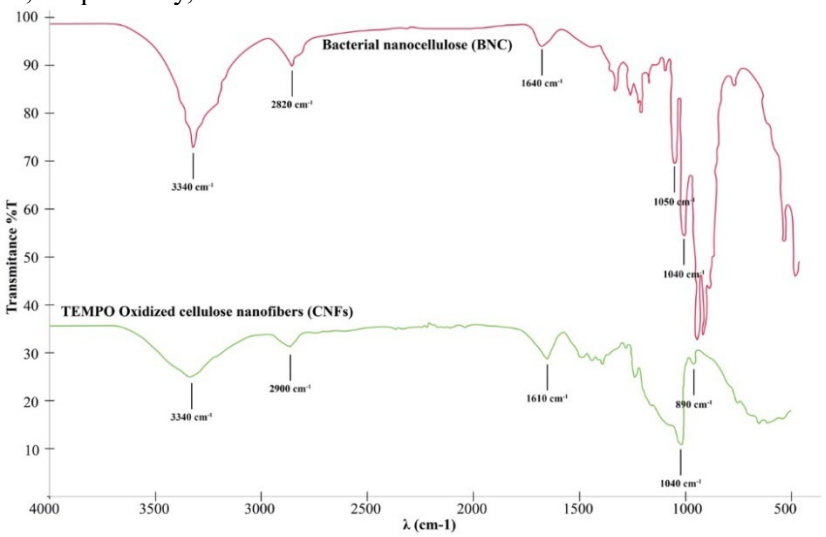

Figure 1: ATR-FTIR spectra of BNC and CNF

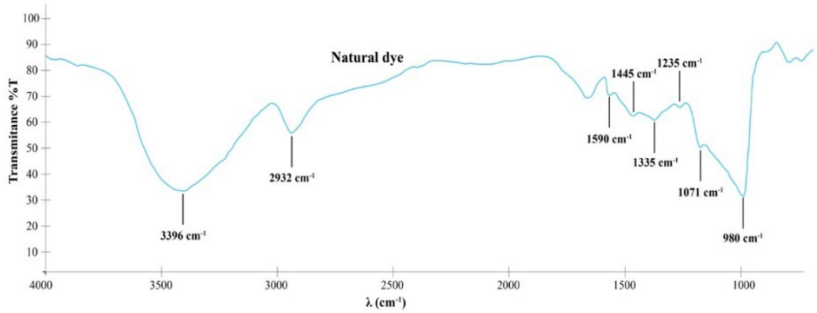

Figure 2: ATR-FTIR spectra of natural dye

During degradation, many foods, such as chicken, release molecules that include nitrogen into the surrounding air, shifting the pH to a more basic level. Thus, a pH-sensitive indicator would inform the consumers of food spoilage. The isolated anthocyanins were investigated at various pHs to confirm their pH-sensitive nature. The pH was adjusted using solutions of NaOH and 0.1 mol/L HCl. Figure 3 displays the hues of the anthocyanin solutions that were prepared at various pH levels. It can be noted that the hue varied from reddish in acidic pH, purple in basic pH, to dark gray-green in extremely basic conditions.

Figure 3 also shows the UV-Vis spectra of the anthocyanins isolated from black carrots at various pH values. A large peak was seen at 530 nm at acidic pH. However, this peak shifted towards 630 nm, as the pH turned basic. In anthocyanins, the protonated form is the flavylium cation, which predominates under acidic conditions (low pH). The flavylium cation is characterized by a positively charged oxygen atom on the hydroxyl group, which is stabilized by the extensive conjugation within the molecular structure. This conjugated system is responsible for the compound's intense absorption in the visible region, typically between 520–550 nm, which corresponds to the red to purple hue observed in anthocyanins under acidic conditions. In low pH environments, the protonation of the oxygen atom at the hydroxyl group stabilizes the flavylium cation form, resulting in strong visible absorption. This contributes to the characteristic coloration of anthocyanins. Upon exposure to basic conditions (higher pH), the flavylium cation undergoes deprotonation, leading to the formation of quinoidal base structures and anionic species,

which exhibit a shift in their UV-Vis absorption spectra. As a result, the visible absorption band is displaced to longer wavelengths, often causing a shift from red or purple to blue or other forms. These findings are consistent with the literature.[54]

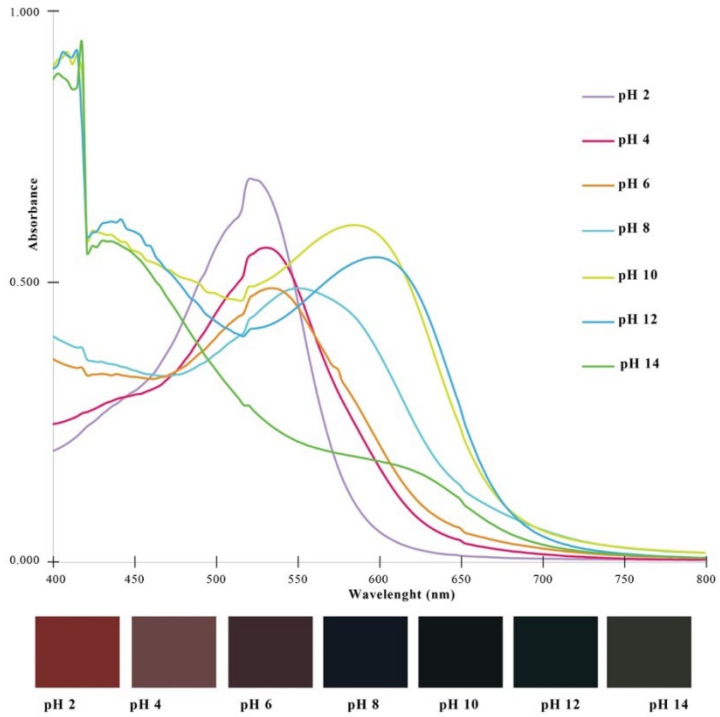

Figure 3: UV-Vis spectra of natural dye solutions at different pH

The total anthocyanin content in the black carrot extract was determined spectrophotometrically to be 469±35 mg/100 g. The results are consistent with the literature.[55]

The anthocyanin solution was used for absorption by the two prepared hydrogels. The chemical structure of the colored hydrogels was examined by ATR-FTIR, and the spectra are given in Figure 4. When examining the spectra, all the peaks belonging to each – anthocyanin, BNC and CNF – are noted. These results show that anthocyanin is physically bound to BNC and CNF, without chemical bonding.[56]

When bacterial nanocellulose (BNC) and cellulose nanofibrils (CNF) were combined with anthocyanins, interactions between the hydroxyl (OH) groups of the nanocelluloses and the anthocyanins led to notable changes in the infrared (IR) spectrum. The OH band in the 3200–3500 cm^{-1} range expanded or shifted, indicating the formation of new hydrogen bonds between the two compounds. Additionally, the presence of BNC or CNF affected the vibrational frequencies of the anthocyanins' functional groups, such as the carbonyl (C=O) and aromatic C-H groups. These interactions resulted in shifts around 1600 cm^{-1} or changes in the intensity of the corresponding bands, suggesting that the nanocellulose influenced the molecular structure of the anthocyanins. These spectral changes provided valuable insights into the nature of the interactions between bacterial nanocellulose, cellulose nanofibrils, and anthocyanins.

The swelling index is a critical parameter for ensuring that natural dyes remain within the hydrogel matrix and for maximizing the functional effect of the active indicator. According to the measurements, a swelling index of 74% for BNC and 67% for CNF was obtained. Although both CNF and BNC are hydrophilic, the results show that CNF exhibits lower water absorption and swelling compared to BNC. This can be attributed to the higher crystallinity of CNF, which restricts water uptake. In contrast, BNC has fewer carboxyl groups and longer fibril lengths, which promote partial agglomeration, disrupt surface smoothness, and facilitate increased water absorption. As a result, BNC exhibits a higher swelling index than CNF, although the overall difference is moderate due to chain entanglements within the BNC

network. These findings are consistent with the literature.[57-60]

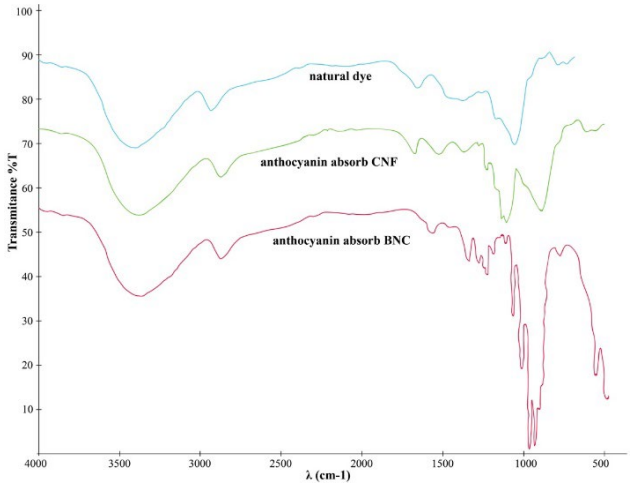

Figure 4: ATR-FTIR spectra of black carrot dye extract, dye extract absorbed into CNF, and dye extract absorbed into BNC

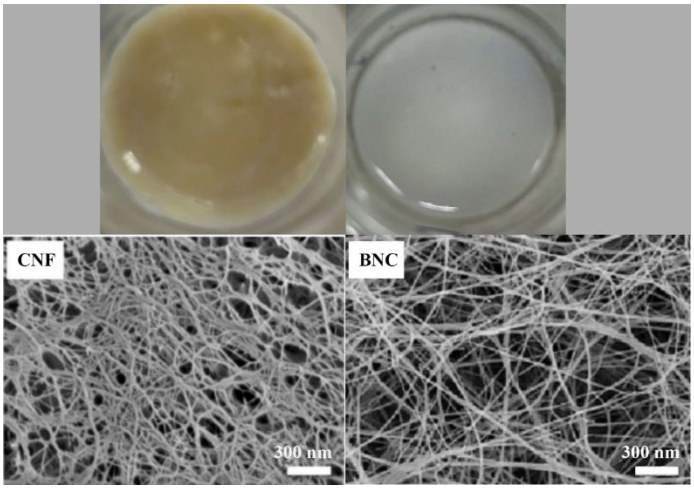

Figure 5: SEM micrographs of CNF and BNC hydrogels

The images and SEM micrographs of the hydrogels obtained from the two different nanocelluloses are given in Figure 5. SEM micrographs reveal that more porous hydrogels are produced from BNC due to its longer fibers. An extensively entangled fibril network, with irregular fibril void arrangement, is noticeable. Meanwhile, CNF hydrogels showed smaller voids. In particular, the width of the voids among the BNC microfibrils were of 300-500 nm, and smaller than 100 nm in CNF. These findings are confirmed in the literature.[61]

Printable hydrogel suspensions were successfully prepared using the obtained anthocyanin-absorbed hydrogels. Screen-printed labels were produced with the prepared hydrogel suspensions without any problems. The color properties of the produced label samples were examined in neutral (room) and basic conditions, and are given in Table 2. It may be remarked that the colors of the smart labels prepared with anthocyanin-absorbed BNC and CNF hydrogels are pink in neutral conditions and blue-green in basic conditions (pH 8-9). It can be clearly seen that the pH change creates a noticeable difference in color. After five repetitions, a similar color change is seen. The flavylium cation, which is predominant in the protonated form of the pigment under acidic conditions, is responsible for the red to purple hue of the compound at acid pH. During exposure to basic conditions (pH 8-9), the flavylium cation undergoes deprotonation, leading

to the formation of quinoidal base structures and anionic species, and the color shifts to purple or blue.

When comparing between the two celluloses, it is noted that the color of the hydrogel suspensions prepared with CNF is a darker pink at the beginning and the color changes clearly after deterioration. This leads to the conclusion that the hydrogel suspension prepared with CNF creates a more basic medium. When the color changes are examined spectrophotometrically, it is determined that there is a color difference of 27 and 34 between room conditions and basic conditions. This difference also reveals that the color difference can be detected spectrally. Such changes have also been remarked by other authors.[62]

Table 2
Color characteristics and images of smart labels

Material	L^*	a^*	b^*	ΔE_{00}	Image
BNC-anthocyanin ink (room conditions)	45	23	2	Reference	
BNC-anthocyanin ink (basic conditions)	44	-2	-7	27	
CNF-anthocyanin ink (room conditions)	38	11	-3	Reference	
CNF-anthocyanin ink (basic conditions)	71	0	-5	34	

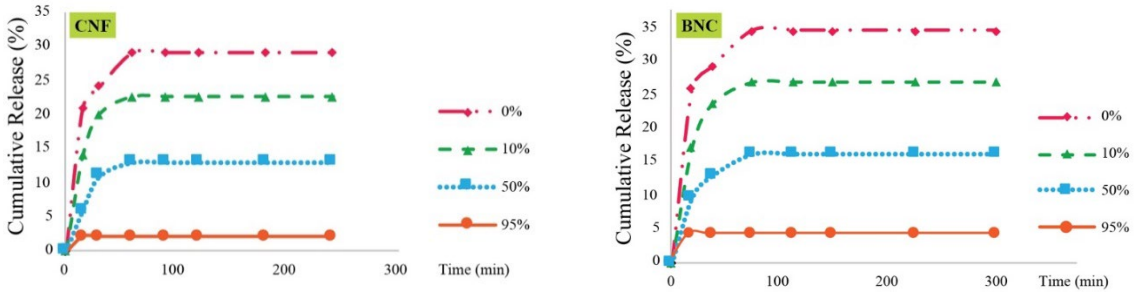

Figure 6: Cumulative release in ethyl alcohol of anthocyanin from smart labels printed with loaded CNF and BNC suspensions

The release of anthocyanin from the CNF and BNC smart labels was examined during immersion of the labels in ethyl alcohol. The anthocyanin absorbed BNC and CNF smart labels presented the same behavior in all simulated solutions: with a burst release during the first 30 min, which then stabilizes during 240 minutes. The cumulative release of anthocyanin-CNF smart labels in 0%, 10%, 50% and 95% ethanol solutions was 29.05%, 22.49%, 12.98% and 2.05%, respectively, and that of the BNC smart labels was 32.35%, 25.29%, 15.13% and 3.85%, respectively. After 65 h, the release of anthocyanin from the CNF and BNC smart labels of immersion in all ethanol solutions reached equilibrium (Fig. 6). Generally, the release of anthocyanin is influenced by the water solubility of the polymer and its swelling ratio. The high swelling of BNC in water could have promoted the

faster release of anthocyanin. Similar results have been reported in the literature.[63] It can be assumed that anthocyanin leakage would be higher from the BNC hydrogel, due to its larger cavities – as the pore size increases, the circulation of anthocyanin becomes easier.

The applicability of the anthocyanin BNC and CNF hydrogel smart labels for determining the degradation of minced beef was examined. It was observed that the color of the label changed gradually over time, and the color change being completed on the 7th day of minced beef storage at +4 °C. These results are consistent with the literature.[32] The color change can be easily perceived by the naked eye. The smart labels containing anthocyanin initially had a pink-purple color and turned to bluish-grey after degradation.

The color changes were also confirmed with the spectrophotometer, ΔE_{00} was measured as 20.55 and 21.44 for anthocyanin BNC and CNF smart labels, respectively. According to ISO 12647-2:2013, a difference of more than 6 between two colors indicates that these are not hues of the same color, and our results fall into this category.

When minced beef deteriorated, nitrogen-derived chemicals were released, which shifted the pH of the medium to a basic pH, and the smart labels changed their color, which could be both visually and spectrally noticeable. These results are consistent with those presented in Table 1. Thus, the two labels were able to successfully determine the deterioration of minced beef (Fig. 7).

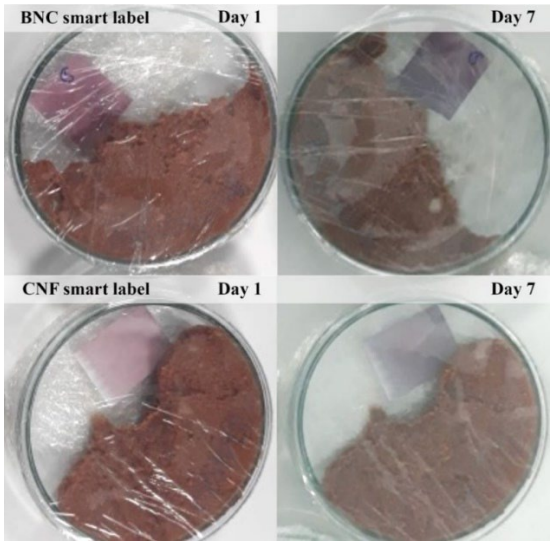

Figure 7: Color change of smart labels produced with anthocyanin-absorbed BNC and CNF hydrogel suspensions during storage of minced beef at +4 °C during 7 days

CONCLUSION

In this study, eco-friendly, smart, and rapid detection labels were successfully developed using anthocyanin-loaded hydrogel suspensions based on bacterial nanocellulose (BNC) and cellulose nanofibrils (CNF). Both BNC and CNF were effectively extracted from natural waste sources, demonstrating the feasibility of valorizing waste materials into high-value products. This approach not only prevents waste generation, but also contributes to environmental sustainability by lowering the overall carbon footprint of the developed system.

Structural and morphological differences between CNF and BNC played a decisive role in the functional properties of the hydrogels. It was determined that CNF exhibited shorter fibril lengths compared to BNC, which directly influenced the swelling capacity of the hydrogels. Specifically, the BNC hydrogel displayed a 15% higher swelling index than CNF, suggesting enhanced fluid uptake capacity and improved compatibility for anthocyanin loading. These findings reveal that BNC provides a more favorable hydrogel matrix for dye incorporation and controlled release.

Anthocyanins were extracted from black carrots, and ATR-FTIR analysis confirmed the presence of cyanidin-3-O-glucoside as the dominant pigment. The pH-responsiveness of the extracted anthocyanin was evidenced by a distinct bathochromic shift in the maximum absorption

wavelength – from 530 nm under acidic conditions to 630 nm under alkaline conditions. This pronounced halochromic behavior underscores the suitability of anthocyanins as natural pH-sensitive indicators in smart packaging systems. Furthermore, quantitative analysis revealed that black carrots contain a substantial anthocyanin concentration – of 469 ± 35 mg/100 g, confirming their potential as a sustainable and abundant natural dye source.

Hydrogels produced from BNC and CNF were successfully impregnated with anthocyanins, and these were subsequently used to prepare printable hydrogel suspensions. Printing trials were carried out without technical difficulties, and the resulting hydrogel-based suspensions yielded mechanically stable, visually distinct, and reproducible smart labels. When these labels were applied to monitor minced beef spoilage, a clear and perceivable color transition from pink/purple to blue/green was observed on the seventh day of storage, directly correlating with microbial spoilage progression. This strong visual signal provides consumers with a reliable, user-friendly, and non-invasive means of monitoring food freshness.

Overall, these results highlight that anthocyanin-loaded BNC and CNF hydrogels represent a promising platform for developing natural, sustainable, and scalable smart packaging technologies. The findings further suggest that BNC hydrogels, due to their superior swelling behavior, may serve as more effective carriers compared to CNF. Beyond meat freshness monitoring, this strategy could be extended to other perishable food products, offering a versatile solution for real-time food quality assessment. Future research could focus on improving color visibility through mordanting techniques and exploring alternative natural halochromic compounds within similar hydrogel matrices, thereby broadening the applicability of this eco-friendly approach in intelligent packaging.

ACKNOWLEDGMENTS: This study has been supported by The Scientific and Technological Research Council of Turkey (TÜBİTAK) and 2508 - Slovenian Research Agency (ARRS) Bilateral Cooperation Program through Project 122N310.

REFERENCES

[1] E. Taherkhani, M. Moradi, H. Tajik, R. Molaei and P. Ezati, *Int. J. Biol. Macromol.*, **164**, 2632 (2020), https://doi.org/10.1016/j.ijbiomac.2020.08.177

[2] M. Ziyaina, B. Rasco, T. Coffey, G. Ünlü and S. S. Sablani, *Food Control*, **100**, 220 (2019), https://doi.org/10.1016/j.foodcont.2019.01.018

[3] P. Ezati, H. Tajik and M. Moradi, *Sens. Actuators B: Chem.*, **285**, 519 (2019), https://doi.org/10.1016/j.snb.2019.01.089

[4] S. Limbo, L. Torri, N. Sinelli, L. Franzetti and E. Casiraghi, *Meat Sci.*, **84**, 129 (2010), https://doi.org/10.1016/j.meatsci.2009.08.035

[5] E. Young, M. Mirosa and P. Bremer, *Front. Sustain. Food Syst.*, **4**, 63 (2020), https://doi.org/10.3389/fsufs.2020.00063

[6] C. E. Realini and B. Marcos, *Meat Sci.*, **98**, 404 (2014), https://doi.org/10.1016/j.meatsci.2014.06.031

[7] J. M. Lagaron, R. Catalá and R. Gavar, *J. Mater. Sci. Technol.*, **20**, 1 (2004), https://doi.org/10.1179/026708304225010442

[8] M. Moradi, H. Tajik, H. Almasi, M. Forough and P. Ezati, *Carbohyd. Polym.*, **222**, 115030 (2019), https://doi.org/10.1016/j.carbpol.2019.115030

[9] P. Müller and M. Schmid, *Foods*, **8**, 16 (2019), https://doi.org/10.3390/foods8010016

[10] K. B. Biji, C. N. Ravishankar, C. O. Mohan and T. K. Srinivasa Gopal, *J. Food Sci. Technol.*, **52**, 6125 (2015), https://doi.org/10.1007/s13197-015-1766-7

[11] A. Barska and J. Wyrwa, *Czech J. Food Sci.*, **35**, 1 (2017), https://doi.org/10.17221/268/2016-CJFS

[12] H. Du, X. Sun, X. Chong, M. Yang, Z. Zhu *et al.*, *Trends Food Sci. Technol.*, **141**, 104200 (2023), https://doi.org/10.1016/j.tifs.2023.104200

[13] J. Zhang, X. Zou, X. Zhai, X. Huang, C. Jiang *et al.*, *Food Chem.*, **272**, 306 (2019), https://doi.org/10.1016/j.foodchem.2018.08.041

[14] X. Zhai, J. Shi, X. Zou, S. Wang, C. Jiang *et al.*, *Food Hydrocoll.*, **69**, 308 (2017), https://doi.org/10.1016/j.foodhyd.2017.02.014

[15] S. Pourjavaher, H. Almasi, S. Meshkini, S. Pirsa and E. Parandi, *Carbohyd. Polym.*, **156**, 193 (2017), https://doi.org/10.1016/j.carbpol.2016.09.027

[16] L. Prietto, T. C. Mirapalhete, V. Z. Pinto, J. F. Hoffmann, N. L. Vanier *et al.*, *LWT*, **80**, 492 (2017), https://doi.org/10.1016/j.lwt.2017.03.006

[17] B. Kuswandi, A. Restyana, A. Abdullah, L. Y. Heng and M. Ahmad, *Food Control*, **25**, 184 (2012), https://doi.org/10.1016/j.foodcont.2011.10.008

[18] B. Liu, H. Xu, H. Zhao, W. Liu, L. Zhao *et al.*, *Carbohyd. Polym.*, **157**, 842 (2017), https://doi.org/10.1016/j.carbpol.2016.10.067

[19] M. Koosha and S. Hamedi, *Prog. Org. Coat.*, **127**, 338 (2019), https://doi.org/10.1016/j.porgcoat.2018.11.028

[20] S. Huang, Y. Xiong, Y. Zou, Q. Dong, F. Ding *et al.*, *Food Hydrocoll.*, **90**, 198 (2019), https://doi.org/10.1016/j.foodhyd.2018.12.009

[21] E. Jamróz, P. Kulawik, P. Krzyściak, K. Talaga-Ćwiertnia and L. Juszczak, *Int. J. Biol. Macromol.*, **122**, 745 (2019), https://doi.org/10.1016/j.ijbiomac.2018.11.008

[22] D. B. Rodriguez-Amaya, *Food Res. Int.*, **124**, 200 (2019), https://doi.org/10.1016/j.foodres.2018.05.028
[23] S. Singh, K. K. Gaikwad and Y. S. Lee, *Korean J. Food Sci. Technol.*, **24**, 167 (2018), https://doi.org/10.20909/kopast.2018.24.3.167
[24] W. Chi, L. Cao, G. Sun, F. Meng, C. Zhang *et al*., *J. Clean Prod.*, **244**, 118862 (2020), https://doi.org/10.1016/j.jclepro.2019.118862
[25] Q. Ma and L. Wang, *Sens. Actuators B: Chem.*, **235**, 401 (2016), https://doi.org/10.1016/j.snb.2016.05.107
[26] M. Kurek, L. Hlupić, M. Ščetar, T. Bosiljkov and K. Galić, *J. Food Sci.*, **84**, 2490 (2019), https://doi.org/10.1111/1750-3841.14716
[27] Q. Ma, Y. Ren, Z. Gu and L. Wang, *J. Clean Prod.*, **166**, 851 (2017), https://doi.org/10.1016/j.jclepro.2017.08.099
[28] S. Mohammadalinejhad, H. Almasi and M. Moradi, *Food Control.*, **113**, 107169 (2020), https://doi.org/10.1016/j.foodcont.2020.107169
[29] M. M. Goodarzi, M. Moradi, H. Tajik, M. Forough, P. Ezati *et al*., *Int. J. Biol. Macromol.*, **153**, 240 (2020), https://doi.org/10.1016/j.ijbiomac.2020.03.014
[30] F. E. Tirtashi, M. Moradi, H. Tajik, M. Forough, P. Ezati *et al*., *Int. J. Biol. Macromol.*, **136**, 920 (2019), https://doi.org/10.1016/j.ijbiomac.2019.06.148
[31] F. He, N. N. Liang, L. Mu, Q. H. Pan, J. Wang *et al*., *Molecules*, **17**, 1571 (2012), https://doi.org/10.3390/molecules17021571
[32] H. Z. Chen, M. Zhang, B. Bhandari and C. H. Yang, *Food Hydrocoll.*, **100**, 105438 (2020), https://doi.org/10.1016/j.foodhyd.2019.105438
[33] H. Z. Chen, M. Zhang, B. Bhandari and Z. Guo, *Postharvest Biol. Technol.*, **140**, 85 (2018), https://doi.org/10.1016/j.postharvbio.2018.02.011
[34] J. S. Lyu, I. Choi, K. S. Hwang, J. Y. Lee, J. Seo *et al*., *Sens. Actuators B: Chem.*, **282**, 359 (2019), https://doi.org/10.1016/j.snb.2018.11.073
[35] C. Rukchon, A. Nopwinyuwong, S. Trevanich, T. Jinkarn and P. Suppakul, *Talanta*, **130**, 547 (2014), https://doi.org/10.1016/j.talanta.2014.07.048
[36] A. Mills and G. A. Skinner, *Analyst*, **135**, 1912 (2010), https://doi.org/10.1039/C000688B
[37] D. Kim, S. Lee, K. Lee, S. Baek and J. Seo, *Food Biotechnol.*, **26**, 37 (2017), https://doi.org/10.1007/s10068-017-0005-6
[38] A. Beyler Çiğil, O. Aydın Urucu, H. Birtane and M. V. Kahraman, *Cellulose*, **28**, 6439 (2021), https://doi.org/10.1007/s10570-021-03932-5
[39] C. Chang and L. Zhang, *Carbohyd. Polym.*, **84**, 40 (2011), https://doi.org/10.1016/j.carbpol.2010.12.023
[40] H. Du, W. Liu, M. Zhang, C. Si, X. Zhang *et al*., *Carbohyd. Polym.*, **209**, 130 (2019), https://doi.org/10.1016/j.carbpol.2019.01.020
[41] P. Lu, M. Guo, Z. Xu and M. Wu, *Coatings*, **8**, 207 (2018), https://doi.org/10.3390/coatings8060207
[42] J. Wang, D. J. Gardner, N. M. Stark, D. W. Bousfield, M. Tajvidi *et al*., *ACS Sustain. Chem. Eng.*, **6**, 49 (2018), https://doi.org/10.1021/acssuschemeng.7b03523
[43] P. Lu, Y. Yang, R. Liu, X. Liu, J. Ma *et al*., *Carbohyd. Polym.*, **249**, 116831 (2020), https://doi.org/10.1016/j.carbpol.2020.116831
[44] G. Lavric, D. Medvescek and M. Skocaj, *Tappi J.*, **19**, 197 (2020), https://doi.org/10.32964/TJ19.4.197
[45] T. Saito, S. Kimura, Y. Nishiyama and A. Isogai, *Biomacromolecules*, **8**, 2485 (2007), https://doi.org/10.1021/bm0703970
[46] F. Dranca and M. Oroian, *Ultrason. Sonochem.*, **31**, 637 (2016), https://doi.org/10.1016/j.ultsonch.2015.11.008
[47] W. Wang and S. Fu, *Cellulose*, **27**, 1009 (2020), https://doi.org/10.1007/s10570-019-02853-8
[48] M. R. Luo, G. Cui and B. Rigg, *Color Res. Appl.*, **26**, 340 (2001), https://doi.org/10.1002/col.1049
[49] B. Kuswandi and A. Nurfawaidi, *Food Control*, **82**, 91 (2017), https://doi.org/10.1016/j.foodcont.2017.06.028
[50] T. Saito, Y. Nishiyama, J. L. Putaux, M. Vignon and A. Isogai, *Biomacromolecules*, **7**, 1687 (2006), https://doi.org/10.1021/bm060154s
[51] A. Isogai, T. Saito and H. Fukuzumi, *Nanoscale*, **3**, 71 (2011), https://doi.org/10.1039/C0NR00583E
[52] Y. Habibi, L. A. Lucia and O. J. Rojas, *Chem. Rev.*, **110**, 3479 (2010), https://doi.org/10.1021/cr900339w
[53] G. Espinosa-Acosta, A. L. Ramos-Jacques, G. A. Molina, J. Maya-Cornejo, R. Esparza *et al*., *Molecules*, **23**, 2744 (2018), https://doi.org/10.3390/molecules23112744
[54] S. Roy and J. W. Rhim, *Crit. Rev. Food Sci. Nutr.*, **61**, 2297 (2021), https://doi.org/10.1080/10408398.2020.1776211
[55] S. Suzme, D. Boyacioglu, G. Toydemir and E. Capanoglu, *Int. J. Food Sci.*, **49**, 819 (2014), https://doi.org/10.1111/ijfs.12370
[56] X. Meng, Q. Shen, T. Song, H. Zhao, Y. Zhang *et al*., *Foods*, **12**, 2602 (2023), https://doi.org/10.3390/foods12132602
[57] B. Joseph, V. K. Sagarika, C. Sabu, N. Kalarikkal and S. Thomas, *J. Bioresour. Bioprod.*, **5**, 223 (2020), https://doi.org/10.1016/j.jobab.2020.10.001
[58] Q. Qin, X. Zhang, B. Gao, W. Liu, L. Han *et al*., *Int. J. Biol. Macromol.*, **257**, 127944 (2024), https://doi.org/10.1016/j.ijbiomac.2023.127944
[59] A. A Oun and J. W. Rhim, *Carbohyd. Polym.*, **127**, 101 (2015), https://doi.org/10.1016/j.carbpol.2015.03.073
[60] B. Kuswandi, N. P. Asih, D. K. Pratoko, N. Kristiningrum and M. Moradi, *Packag. Technol.*, **33**, 321 (2020), https://doi.org/10.1002/pts.2507
[61] G. Zubova, H. Melnyk, I. Zaets, T. Sergeyeva, O. Havryliuk *et al*., *Polymers*, **16**, 2327 (2024), https://doi.org/10.3390/polym16162327
[62] H. Wang, B. Li, F. Ding and T. Ma, *Prog. Org. Coat.*, **149**, 105921 (2020), https://doi.org/10.1016/j.porgcoat.2020.105921
[63] M. Cheng, X. Yan, Y. Cui, M. Han, Y. Wang *et al*., *Polym. J.*, **14**, 1214 (2022), https://doi.org/10.3390/polym14061214